JOURNAL OF MATERIALS SCIENCE 23 (1988) 1539–1546

# Preparation and thermal evolution of sol–gel derived transparent $ZrO_2$ and $MgO–ZrO_2$ gel monolith

P. KUNDU, D. PAL, SUCHITRA SEN
*Central Glass and Ceramic Research Institute, Calcutta 700 032, India*

Transparent gel monoliths of pure and MgO-doped zirconia having dopant concentrations in the range 0 to 15 mol% were prepared by chemical polymerization of zirconium n-propoxide and magnesium acetate tetrahydrate using 2-methoxy ethanol as solvent. The thermal evolution of amorphous gels was studied by differential thermal analysis, X-ray diffraction and transmission electron microscopy. The crystallization of pure and doped zirconia gels occurred in the temperature range 360 to 450° C. The first crystalline phase to appear is tetragonal for pure and 2 mol% doped zirconia, and cubic for 3 to 15 mol% doped samples. Both crystallization and decomposition temperatures are found to increase with increasing dopant concentration, approaching a saturation value for 10 mol% doped samples. It has been established that the transformation of the cubic to the monoclinic phase takes place via a metastable tetragonal phase. A linear relationship between the lattice parameter of cubic zirconia and MgO concentration has been established. X-ray diffraction studies have also revealed that the entire amount of MgO used in preparing doped zirconia gels remains in a single $MgO–ZrO_2$ crystalline phase formed initially by thermal treatment.

## 1. Introduction

Pure zirconia has three polymorphic forms: cubic, tetragonal and monoclinic. At room temperature zirconia is monoclinic, which changes to a tetragonal form above 1170° C and finally to a cubic fluorite phase above 2300° C. The addition of certain oxides such as MgO, CaO and $Y_2O_3$ stabilizes the high-temperature cubic phase of zirconia to retain a single phase at lower temperatures. The aliovalent ions substitute for zirconium ions in the cubic phase and produce oxygen vacancies which enhance the ionic conductivity. Cubic stabilized zirconia ceramic, as a solid electrolyte, finds application in electrochemical devices: fuel elements, oxygen analyser sensors, electrolysers for water vapour, oxygen monitors, oxygen pumps, etc. [1–3].

For the last twenty years the alkoxide decomposition (thermal or hydrolytic) process has been widely used in preparing stabilized zirconia ceramics [4–9]. Oxide powders derived from alkoxides have a high sintering capacity and require a low concentration of additives to stabilize the cubic phase [4]. The particle size and shape and size distribution of such powders, which are very fine and agglomerated, were not controlled in these early studies. In this regard, considerable attention has been paid to synthesize monosized pure and doped zirconia powders by the controlled hydrolysis of alkoxides [10, 11]. Such monosized spheroidal particles with a high packing density can be sintered to fine-grained ceramics with > 98% theoretical density at 1160° C [11]. However, no attempt has been made so far to prepare stabilized zirconia ceramic from gel monoliths obtained by the chemical polymerization of alkoxides.

A study of the thermal evolution of gel monoliths is needed in order to follow the development, growth and "destabilization" (decomposition) of the crystalline phases formed during heating of the amorphous gel phase. Many workers have described the thermal behaviour of zirconia [12–19], magnesia–zirconia [19, 20] and yttria–zirconia [4, 21] gel powders obtained from the hydrolysis of inorganic salts and alkoxides. The thermal and crystallization behaviours of doped zirconia gel monoliths have not yet been reported.

The object of the present investigation is the preparation and characterization of stabilized zirconia solid electrolyte in the form of monoliths, thin films and fibres using the sol–gel technique. As a first step we have successfully developed a method of preparing magnesia-doped zirconia transparent gel monoliths. The present communication reports the preparation and thermal evolution of these monoliths using differential thermal analysis (DTA), X-ray diffraction (XRD) and electron diffraction in the transmission electron microscope (TEM).

## 2. Experimental procedure

### 2.1. Gel preparation

Technical grade zirconium n-propoxide (Fluka, Switzerland), GR grade magnesium acetate tetrahydrate $Mg(OOCCH_3)_2 \cdot 4H_2O$ (Merck, Germany) and synthesis grade 2-methoxy ethanol (methyl cellosolve) $C_3H_8O_2$, (Merck, India) were used for pure and MgO-doped zirconia gel preparation. In a Pyrex

0022–2461/88 $03.00 + .12 

beaker, 30 g of zirconium n-propoxide was dissolved in 70 ml of methyl cellosolve. In the case of MgO-doped $ZrO_2$ samples, the required weights of magnesium acetate tetrahydrate dissolved in methyl cellosolve were added dropwise from a burette to a solution of zirconium alkoxide in methyl cellosolve whilst stirring continuously with a Teflon-coated magnetic stirrer. Eight samples of different dopant concentration were prepared. Samples M0, M2, M3, M4, M5, M7, M10 and M15 contained 0, 2, 3, 4, 5, 7, 10 and 15 mol % MgO, respectively. The solution mixtures were poured into Pyrex beakers, covered with polythene sheets and kept in the atmosphere to form stiff gels. Transparent (almost colourless, with slight yellowish tint) gel monoliths were formed in 7 to 10 days, depending on the temperature and the relative humidity of the atmosphere.

### 2.2. Drying and firing of gel

Monolithic gels derived from the solution were allowed to dry at room temperature for 4 to 5 weeks. Drying was nearly completed at 130° C in an air oven. These dried gels were crushed, ground into powders and sieved through 200 B.S. mesh (opening 0.075 mm). Heat-treatment of the gel powders was performed in air at several different temperatures between 320 and 1000° C. Grinding was not conducted after heat-treatment to avoid stress-induced transformation of the tetragonal $ZrO_2$ [22, 23].

At each run, eight powders of different compositions (M0 to M15) were kept in a Kanthal-wired electrically heated furnace; the heating zone was approximately 18 in. × 12 in. × 10 in. (46 cm × 30 cm × 25 cm). Samples were placed in the uniform-temperature zone for similar thermal treatment. The heating rate was adjusted to attain 300° C after 18 h, subsequently heated from 300° C to the preselected ultimate temperature at the rate of 100° C $h^{-1}$ and maintained for 1 h at that temperature.

### 2.3. Differential thermal analysis

The thermal analysis was carried out with a Shimadzu thermoanalyser in air. 40 mg of dried gel powder was placed in a platinum crucible and heated at the rate of 10° C $min^{-1}$. Finely powdered alumina was used as a reference material.

### 2.4. X-ray diffraction

Powder diffraction patterns were obtained by using a Philips PW1730 X-ray diffraction unit employed with nickel-filtered Cu$K\alpha$ radiation. The crystallite size of the tetragonal or cubic $ZrO_2$ was calculated by the Scherrer formula, $D = K\lambda/\beta \cos\theta$, with $K = 0.9$ [18], where $\lambda$ is the wavelength (Cu$K\alpha$), $\theta$ the diffraction angle used and $\beta$ the line broadening of the (1 1 1) diffraction peak. The corrected half-width, $\beta$, of the diffraction peak using Klug and Alexander's method [24] is $\beta = (B_{obs}^2 - b^2)^{1/2}$ where $B_{obs}$ and $b$ are the observed line-widths at half-peak intensity of crystalline $ZrO_2$ and $\alpha$-quartz, respectively. The (1 0 1) diffraction peak of $\alpha$-quartz was used as the reference for instrumental broadening. Itoh [25] has demonstrated that the line broadening in precipitated hydrous zirconia is due to a crystallite size effect. Following his method of analysis we have found that the line broadening in our sample has a similar origin.

For lattice parameter determination of the cubic phase, the peak positions were obtained precisely by chart-recording at a scanning speed of 0.25° $(2\theta)$ $min^{-1}$ and a chart speed of 1 cm $min^{-1}$. Accurate estimations of the peak positions were done by extrapolation of the centres of section lines drawn parallel to the background level towards the top of the symmetric peak [26]. The angular positions for 1 1 1, 2 0 0, 2 2 0, 3 1 1 and 4 0 0 peaks for the cubic phase were obtained with an accuracy of $\pm 0.025°$ $(2\theta)$. An extrapolation of the lattice parameter values of the above crystallographic planes using a least-squares fit to $\cos\theta \cot\theta = 0$ gives the true lattice parameter $a_0$.

### 2.5. Electron diffraction

The TEM was also used to take selected-area diffraction patterns for the detection and identification of the trace amount of a second phase precipitated from cubic zirconia with progressive heat-treatment. A Jeol 200 kV TEM was used for this purpose. Powder samples were dispersed on carbon-coated 200-mesh grids and examined at 160 kV in the TEM.

## 3. Results and discussion

### 3.1. Gel formation and monolithicity of gels

Zirconium alkoxide is readily hydrolysed to oxides containing aquo-groups [27] causing precipitates. It is very difficult to add water to this system. Under controlled conditions and with a limited amount of water, the hydrolysis and polycondensation result in the formation of soluble polymeric oxide–alkoxides, $ZrO_x(OR)_{4-x}$ [28, 29]. Ganguli and Kundu [30] observed that transparent sols and coatings were produced by the controlled hydrolysis of zirconium propoxide solution containing a maximum of 2.5 wt % $ZrO_2$ when isopropanol was used as solvent. The controlled hydrolysis of more concentrated alcoholic solutions containing higher equivalent amounts of $ZrO_2$ results in the formation of precipitates. Recently Kundu and Ganguli [31] have succeeded in preparing transparent gel monoliths by the hydrolysis of zirconium propoxide in a non-polar solvent containing up to 10 wt % equivalent $ZrO_2$ content.

In this work, the slow hydrolysis of zirconium n-propoxide in methyl cellosolve by atmospheric moisture leads to the formation of transparent monolithic gels. The equivalent $ZrO_2$ concentration is ~ 12 wt %. In the case of MgO-doped gel monoliths, the addition of MgO as magnesium acetate invariably results in the formation of transparent sols and this remains so throughout the period of hydrolytic polycondensation reactions. The hydrolysis of zirconium alkoxides containing magnesium acetate is not well understood, and is more complex than in the pure $ZrO_2$ system. Probably, magnesium ions are uniformly distributed on the pore surfaces of the zirconia gel structure [32]. During heating, magnesium ions substitute for zirconium ions in the crystal structure forming stabilized cubic or tetragonal zirconia.

The transparent monolithic dried gel could only be


*Figure 1* Transparent 10 mol % $MgO-ZrO_2$ dried gel monolith.

prepared under extremely slow-drying conditions. It was observed that cracks developed even in a fairly dry gel sample when it was suddenly exposed to air. Good results were obtained when the gel was dried over a period of 4 weeks or more. The dry gels so obtained had a bulk density of $\sim 3\,g\,cm^{-3}$. The linear shrinkage was 75 to 85%. A photograph of a transparent monolithic dried gel sample is shown in Fig. 1.

The preparation method using cellosolve as solvent and acetate as dopant has the special advantage that the sols remain transparent over a wide range of equivalent oxide concentration. Thus this method is well suited for the preparation of thin films and fibres. Preliminary experiments on thin films give encouraging results.

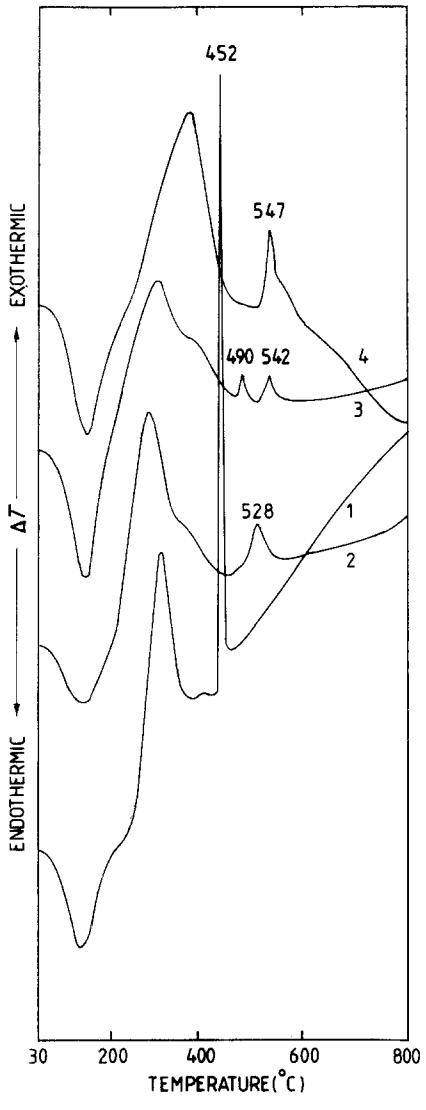


*Figure 2* DTA curves of 130° C dried pure and MgO-doped $ZrO_2$ gel: (1) M0 (pure $ZrO_2$), (2) M2 (2 mol % MgO), (3) M5 (5 mol % MgO) and (4) M10 (10 mol% MgO).

## 3.2. Thermal analysis

DTA curves of 130° C dried pure and magnesia-doped zirconia (M0, M2, M5 and M10) powders are depicted in Fig. 2. The curves for all the samples exhibit some common features. They all show an endothermic peak at 120 to 150° C associated with the removal of water and organic solvents. The other feature of these curves is a broad exothermic peak in the range 300 to 400° C followed by another exothermic peak. XRD patterns of samples collected from the first exothermic peak temperature show a typical amorphous halo pattern. Therefore, the first exotherm is not due to crystallization and is assigned to the decomposition and burning of organics. Samples taken from the second peak temperature show the presence of cubic or tetragonal zirconia depending upon the dopant concentration. The crystalline phase obtained from the second exothermic peak is tetragonal for M0 and M2 whereas the phase is cubic for M5 and M10.

In the case of pure zirconia gel, a glow phenomenon was found to occur at the second exothermic peak (452° C). XRD reveals the presence of tetragonal phase at the glow exotherm. This is further supported by the fact that the dark grey powder collected at the glow temperature gains in weight and regains its white colour on reheating. Livage *et al.* [19] deduced that the original black powder has the non-stoichiometric formula $ZrO_{1.96}$. The glow phenomenon associated with the crystallization of pure zirconia has also been observed by others [16, 33]. DTA curves for samples other than pure zirconia powder do not exhibit a glow phenomenon and this may be possibly due to magnesium ions which stabilize the metastable zirconia phases. In the case of M5 gel powder, beside the second exothermic peak, an additional peak has been observed. The origin of this peak is not known but may be due to the removal of defects as suggested by Osendi *et al.* [18]. The DTA curves shown in Fig. 2 and XRD (discussed later) show an inhibiting effect of MgO on crystallization, consistent with the prediction of Polezhaev [34] and Livage *et al.* [19].

## 3.3. X-ray and electron diffraction

XRD was used to study phase transformation, crystal growth and the variation of lattice parameter with dopant concentration. Fig. 3 shows the XRD patterns of pure and MgO-doped $ZrO_2$ samples (M0, M2, M4 and M10). It is seen from the figure that the respective crystallization temperatures are 360, 380, 400 and 450° C. The increase in the crystallization temperature with dopant concentration is quite consistent with the DTA results. The first crystallization phase in the case of M0 and M2 is tetragonal and for the rest of the samples cubic. It is further evident from Fig. 3 that the stability of doped zirconia increases with an increase in dopant concentration and reaches a maximum for M10. It is observed that the stability did not improve

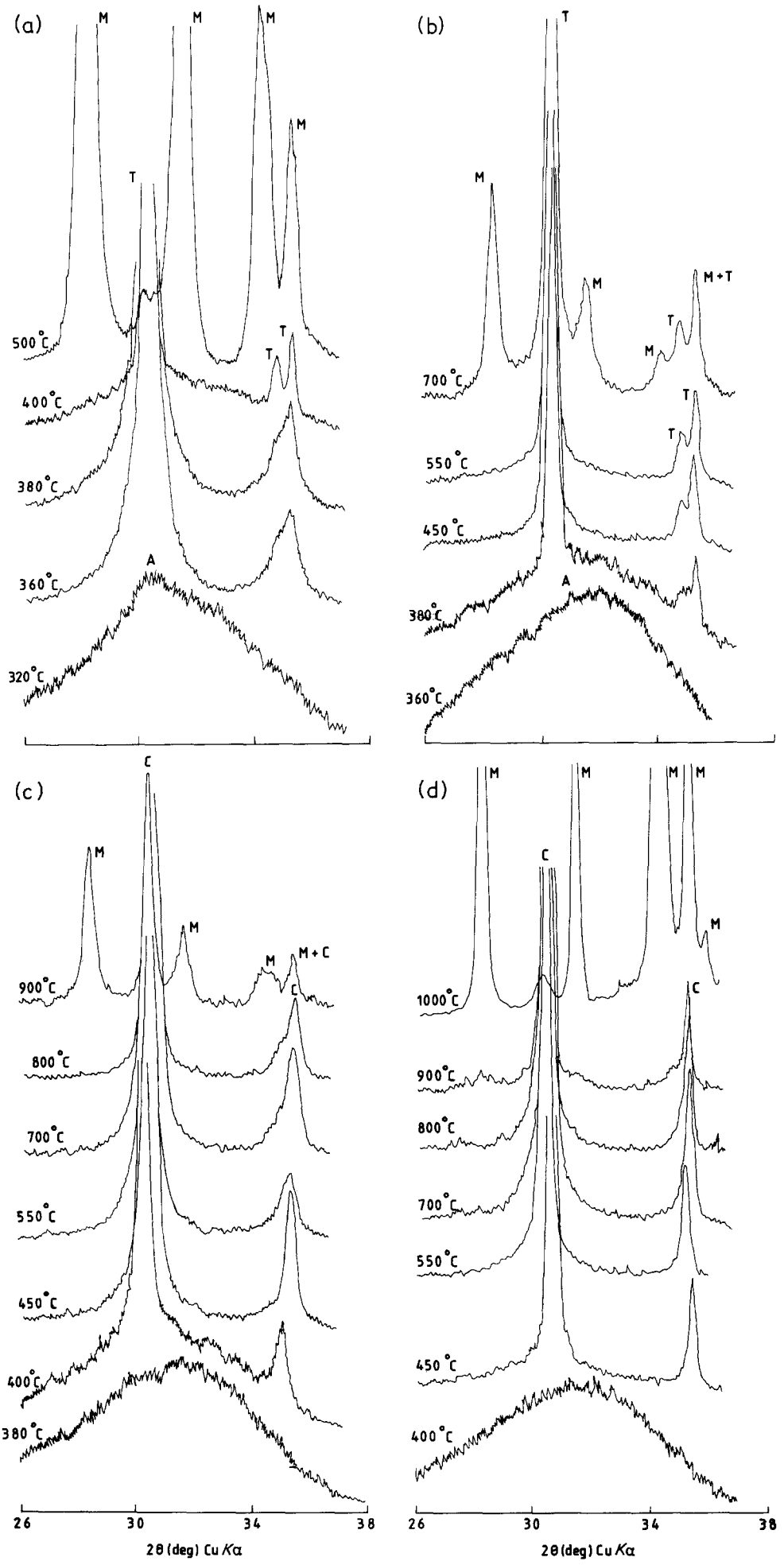


*Figure 3* X-ray diffraction patterns of pure and MgO-doped $ZrO_2$ gels heated for 1 h at temperatures indicated: (a) M0 (pure $ZrO_2$), (b) M2 (2 mol % MgO), (c) M4 (4 mol % MgO) and (d) M10 (10 mol % MgO). M = monoclinic, T = tetragonal, C = cubic.

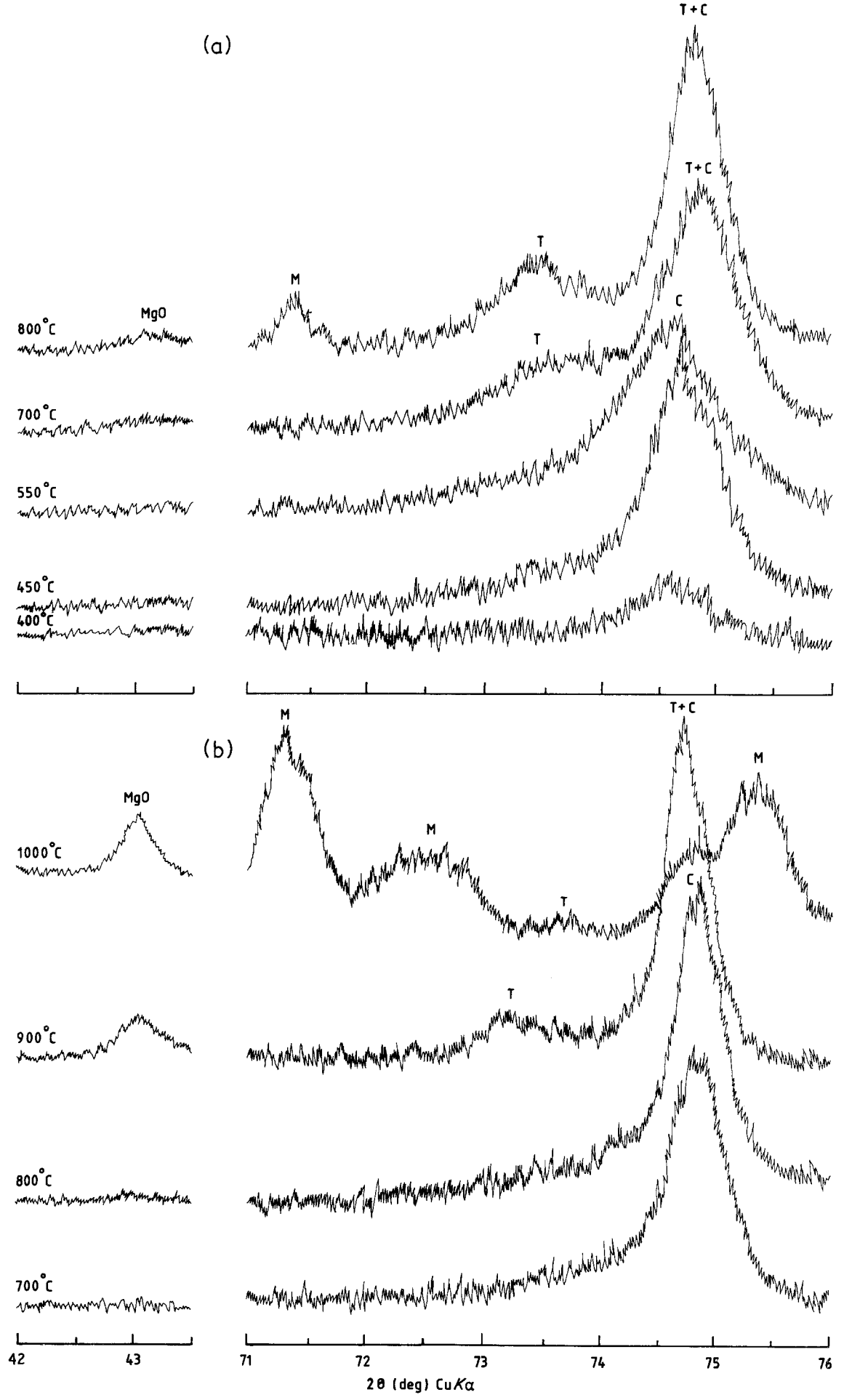


*Figure 4* X-ray diffraction patterns of $MgO–ZrO_2$ gels (a) M4 (4 mol % MgO) and (b) M10 (10 mol % MgO) showing conversion of cubic phase initially formed to monoclinic and MgO, through an intermediate tetragonal phase at temperatures indicated for 1 h. M = monoclinic, T = tetragonal, C = cubic.

TABLE I Average crystallite size for tetragonal and cubic zirconia calculated by using the (1 1 1) diffraction peak at various temperatures

| Sample | Composition (mol %) | | Average crystallite size (nm)* | | | | | | | | |
|---|---|---|---|---|---|---|---|---|---|---|---|
| | MgO | $ZrO_2$ | 360° C | 380° C | 400° C | 450° C | 550° C | 700° C | 800° C | 900° C | 1000° C |
| M0 | 0 | 100 | 18.2(T) | 23.3(T) | 25.0(T) | 29.1(T) | – | – | – | – | – |
| M2 | 2 | 98 | A | 21.5(T) | 23.3(T) | 24.9(T) | 26.2(T) | 28.5(T) | – | – | – |
| M3 | 3 | 97 | A | A | 20.0(C) | 24.5(C) | 16.3(C, T) | 17.8(C, T) | 22.3(C, T) | – | – |
| M4 | 4 | 96 | A | A | 19.5(C) | 25.3(C) | 14.9(C, T) | 18.0(C, T) | 24.4(C, T) | – | – |
| M5 | 5 | 95 | A | A | A | 28.0(C) | 30.3(C) | 18.9(C, T) | 24.4(C, T) | – | – |
| M7 | 7 | 93 | A | A | A | 20.3(C) | 25.1(C) | 28.5(C) | 16.7(C, T) | 21.5(C, T) | – |
| M10 | 10 | 90 | A | A | A | 24.1(C) | 25.9(C) | 29.3(C) | 35.7(C) | 26.4(C, T) | 13.1(C, T) |
| M15 | 15 | 85 | A | A | A | 18.2(C) | 21.7(C) | 21.9(C) | 23.5(C) | 22.3(C, T) | 16.7(C, T) |

*A = amorphous, T = tetragonal, C = cubic.

further with increasing the dopant concentration up to 15 mol %. Nevertheless, the M10 sample has a better stability than the 15 mol % MgO-stabilized cubic zirconia obtained by Dongare and Sinha [9]. While the former decomposes to monoclinic zirconia and MgO at 1000° C, the later decomposes completely to monoclinic zirconia and MgO at 900° C.

Figs 3a and b show that with increasing temperature, the diffraction peaks around 30.2° (2$\theta$) for M0 and M2 become narrower and the 0 0 2–2 0 0 doublet separates more, and finally the tetragonal phase transforms to the monoclinic phase. The average crystallite size calculated from the half-width is found to increase with temperature and attains a value of 29.1 nm at 450° C for M0 and 28.5 nm at 700° C for M2 (Table I), when the monoclinic phase is observed. This is close to the critical crystallite size ($\sim$ 30 nm) determined by Garvie [35]. XRD patterns of M4/550° C and M10/900° C (Figs 3c and d, respectively) show anomalous behaviour. Initially the widths of the peaks around 30.4 and 35.3° of heat-treated gel powders decrease with the rise of temperature, but increase at 550 and 900° C for M4 and M10, respectively. Average crystallite sizes of the cubic phase at different temperatures, calculated by making use of the (1 1 1) peak half-width, are shown in Table I. It is striking that, contrary to normal behaviour, the crystal size decreases at 550° C for M4 and at 900° C for M10. One plausible explanation may be that, with a progressive rise in temperature, the cubic phase gradually converts to an intermediate tetragonal phase so that the (1 1 1) peaks of the two phases overlap, thereby broadening the peak.

From a careful study of Figs 3c and d, it is observed that the (2 0 0) peak (35.3 to 35.5° (2$\theta$)) has an ascending asymmetry for M4 heated at 550° C and M10 heated at 900° C. This indicates that at these temperatures, cubic zirconia gradually transforms to another metastable state. Although the 0 0 2–2 0 0 doublet cannot be separated owing to line broadening and/or the presence of a minor amount of the decomposed product formed, the clear asymmetry shown by the apparent single line (2 0 0) may be assigned to a tetragonal lattice [36] which results from decomposition of the cubic phase. A high-angle scan (71 to 76° (2$\theta$) at the rate of 0.25° $min^{-1}$ (Fig. 4) provides further confirmatory evidence of the formation of the tetragonal phase. It shows the appearance of the characteristic $(0\,0\,4)_t$ peak around 73.3° (2$\theta$) at 700° C for M4 and 900° C for M10. However, a low intensity $(0\,0\,4)_t$ peak for M4 cannot be detected at 550° C, probably due to poor crystallinity and/or a minor amount of the tetragonal phase. The $(4\,0\,0)_t$ peak is not revealed. Perhaps it overlaps with $(4\,0\,0)_c$ as it is observed that the $(4\,0\,0)_c$ peak shifts to quite an extent from 74.68° (2$\theta$) for M3 to 75.05° (2$\theta$) for M15. Also, a pertinent observation that may be made from the scan over 42 to 43.5° in Figs 4a and b is that the entire amount of MgO goes into a single cubic MgO–$ZrO_2$ solid solution and MgO precipitates as a crystalline phase simultaneously with the formation of tetragonal phase in M4 (700° C) and M10 (900° C). At higher

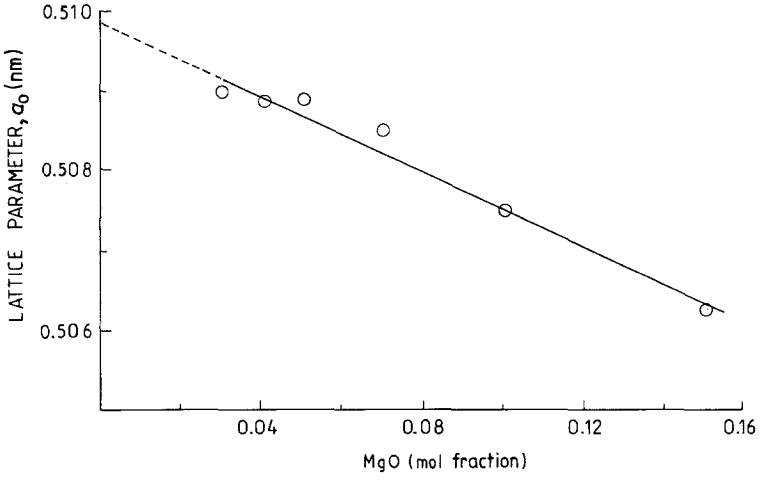


*Figure 5* Concentration dependence of lattice parameters of cubic solid solutions of MgO–$ZrO_2$.

temperatures (800° C for M4 and 1000° C for M10) all three polymorphic phases (cubic, tetragonal and monoclinic) of zirconia and MgO are present. With increasing holding time at these temperatures only monoclinic $ZrO_2$ and MgO are obtained.

From the above findings it may be proposed that c-$ZrO_2$(ss) formed at low temperatures (400 to 450° C) from an MgO–$ZrO_2$ gel decomposes to monoclinic $ZrO_2$ and MgO through an intermediate tetragonal $ZrO_2$(ss). This is in disagreement with observations on the decomposition of hypo-eutectoid [37] and hyper-eutectoid [38] MgO–$ZrO_2$ cubic solid solutions ageing at $\leqslant$ 1200° C, where decomposition follows the reaction

$$\text{c-}ZrO_2(\text{ss}) \rightarrow \text{m-}ZrO_2(\text{ss}) + MgO$$

consistent with the phase diagram suggested by Grain [39]. In the present investigation, probably the small size of the crystallites is responsible for the extension of the stable tetragonal region at the lower temperature [40]. Consequently the decomposition of the cubic phase to the tetragonal phase and MgO takes place in the initial stage. Afterwards, when the crystallites grow appreciably, transformation to the monoclinic phase takes place.

The probable sequence of phase transformations with the thermal evolution of MgO–$ZrO_2$ amorphous gel containing 3 to 15 mol % MgO may be proposed in the following way:

MgO–$ZrO_2$, amorphous gel

↓ 400 to 450° C

cubic zirconia (ss)

↓ 550 to 900° C

tetragonal zirconia (ss) + MgO

↓ 800 to 1000° C

mononclinic zirconia (ss) + MgO

The polymorphic transformation of MgO–$ZrO_2$ solid solution is smooth and continuous. A similar observation was made by Mazdiyasni [41] for pure zirconia powder in high-temperature XRD studies.

The lattice parameter $a_0$ of stabilized cubic $ZrO_2$ is plotted against MgO concentration (expressed as a molar fraction) in Fig. 5 for the 450° C heated samples. The straight line obtained by a least-squares fit method could be described by the following relation:

$$a_0 \text{ (nm)} = 0.5099 - 0.0235X$$

where $X$ is the mole fraction of MgO in the range $0.03 \leqslant X \leqslant 0.15$. Toraya *et al.* [42] obtained a similar equation $a_0 = 0.5105 - 0.0198X$ by a least-squares fit of the literature data [39] for 10 to 15 mol % MgO stabilized zirconia with the intercept constrained to a value of 0.5105 nm. It is worthwhile to mention that data for $a_0$ of cubic $ZrO_2$ in the wide range studied here are not available elsewhere in the literature.

The sequence of phase transformations of the MgO–$ZrO_2$ system, as established from XRD studies, has received further support from transmission electron microscopy, using the selected-area diffraction (SAD) mode. SAD patterns of M10 samples heat-treated at different temperatures are shown in Fig. 6. The diffraction patterns indicate the presence of cubic phase in each of the samples treated at 700, 800 and 900° C (Figs 6a, b and c, respectively). In the case of the third sample (M10/900° C) diffraction spots, characteristics of a metastable tetragonal phase, are also prominently exhibited. A few spots (having negligible intensity) due to the monoclinic phase could also be detected. The SAD pattern of a sample treated at 1000° C (Fig. 6d) reveals that the predominant phase is monoclinic, showing thereby that almost complete conversion of the cubic to the monoclinic phase takes place at 1000° C through a metastable tetragonal phase.

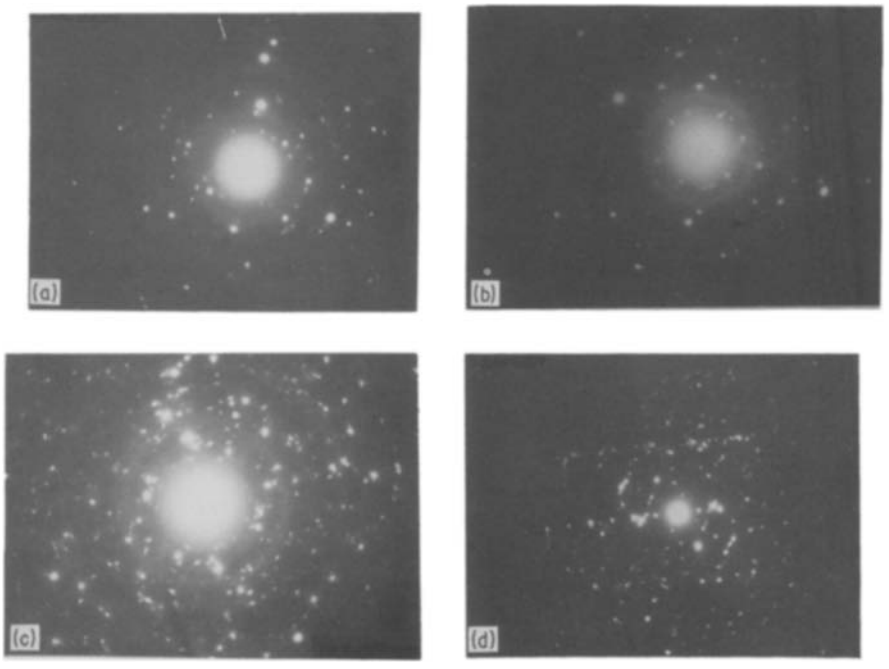


*Figure 6* Selected-area electron diffraction patterns taken at 160 kV of M10 (10 mol % MgO–$ZrO_2$) gels heat-treated for 1 h at (a) 700° C, (b) 800° C, (c) 900° C and (d) 1000° C.

## 4. Conclusions

1. The use of methyl cellosolve as a solvent has the advantage of removing the difficulty associated with the hydrolysis of alcoholic solutions of alkoxides forming precipitates in most cases. Transparent monolithic $ZrO_2$ and $MgO–ZrO_2$ gels can easily be prepared by hydrolysis and polycondensation reactions of zirconium n-propoxide and magnesium acetate tetrahydrate using methyl cellosolve as a solvent.

2. These gels on heat-treatment at 360 to 450° C crystallize to a single phase, this being tetragonal for pure and 2 mol % $MgO–ZrO_2$ and cubic for 3 to 15 mol % $MgO–ZrO_2$ gels.

3. The entire amount of MgO used in preparing $MgO–ZrO_2$ gels remains in a single crystalline $MgO–ZrO_2$ phase before decomposition, indicating that a high degree of homogeneity is achieved during gelling of the sols.

4. The crystallization temperature and the stability of the crystalline phase increase with increasing magnesium content, reaching maxima at 10 mol % MgO.

5. It has been established that the tranformation of the cubic to the monoclinic phase at temperatures $\leqslant 1000°$ C takes place via an intermediate metastable tetragonal phase.

6. A linear relation between the experimentally determined lattice parameter of cubic zirconia and the MgO molar concentration has been obtained for 3 to 15 mol % MgO in $MgO–ZrO_2$ solid solutions.


## Acknowledgements

The authors are grateful to Dr S. Kumar, Director, Central Glass and Ceramic Research Institute, Calcutta for his keen interest in the work and kind permission to publish the paper. The authors are indebted to Dr S. Thiagarajan for constant encouragement and advice. Thanks are also due to Mr D. K. Ghosh and Dr A. K. Chakravorty for performing XRD and DTA. The TEM facility offered by RSIC, Bose Institute, Calcutta for this work is gratefully acknowledged. Finally, the authors wish to thank Mr S. N. Chatterjee for taking photographs.


## References


1. R. V. WILHELM Jr and D. S. EDDY, *Amer. Ceram. Soc. Bull.* **56** (1977) 509.
2. B. C. H. STEELE, J. DRENNAN, R. K. SLOTWINSKI, N. BONANOS and E. P. BUTLER, in "Advances in Ceramics", Vol. 3, edited by A. H. Heuer and L. W. Hobbs (American Ceramic Society, Columbus, Ohio, 1981) p. 286.
3. A. I. IOFFE, M. V. INOZEMTSEV, A. S. LIPILIN, M. V. PERFIL'EV and S. V. KARPACHEV, *Phys. Status Solidi (a)* **30** (1975) 87.
4. K. S. MAZDIYASNI, C. T. LYNCH and J. S. SMITH, *J. Amer. Ceram. Soc.* **50** (1967) 532.
5. M. HOCH, in "Decomposition of Organometallic Compounds to Refractory Ceramics, Metals and Metal-Alloys", Proceedings of International Symposium, 1967 (University of Dayton Press, Dayton, 1968) p. 171.
6. M. HOCH and K. M. NAIR, *Ceramurgia Int.* **2** (1976) 88.
7. M. J. VERKERK, B. J. MIDDELHUIS and A. J. BURGGRAAF, *Solid State Ionics* **6** (1982) 159.
8. N. Ya. TUROVA and M. I. YANOVSKAYA, *Inorg. Mater.* **19** (1983) 625.
9. M. K. DONGARE and A. P. B. SINHA, *J. Mater. Sci.* **19** (1984) 49.
10. B. FEGLEY Jr and E. BARRINGER, in "Better Ceramics Through Chemistry", Materials Research Society Symposia Proceedings Vol. 32, edited by C. J. Brinker (Elsevier, New York, 1984) p. 187.
11. B. FEGLEY Jr, P. WHITE and H. K. BOWEN, *Amer. Ceram. Soc. Bull.* **64** (1985) 1115.
12. K. S. MAZDIYASNI, C. T. LYNCH and J. S. SMITH, *J. Amer. Ceram. Soc.* **49** (1966) 286.
13. M. L. VEIGA BLANCO, M. VALLET REGI, A. MATA ARJONA and E. GUTIERREZ RIOS, *An. Quim. Ser. B* **76** (1980) 218.
14. M. I. DOMNINA and S. K. FILATOV, *Inorg. Mater.* **19** (1983) 828.
15. T. ITOH, *J. Mater. Sci. Lett.* **4** (1985) 1029.
16. G. GIMBLETT, A. A. RAHMAN and K. S. W. SING, *J. Chem. Tech. Biotechnol.* **30** (1980) 51.
17. M. J. TORRALVO, M. A. ALARIO and J. SORIA, *J. Catal.* **86** (1984) 473.
18. M. I. OSENDI, J. S. MOYA, C. J. SERNA and J. SORIA, *J. Amer. Ceram. Soc.* **68** (1985) 135.
19. J. LIVAGE, K. DOI and C. MAZIERES, *ibid.* **51** (1968) 349.
20. N. H. BRETT, M. GONZALEZ, J. BOUILLOT and J. NIEPCE, *J. Mater. Sci.* **19** (1984) 1349.
21. A. I. IOFFE, V. N. STREKALOVSKII, D. S. RUTMAN and S. V. KARPACHEV, *Dokl. Akad. Nauk SSSR* **209** (1973) 646.
22. R. C. GARVIE, R. H. HANNINK and R. T. PASCOE, *Nature* **258** (1975) 703.
23. T. K. GUPTA, F. F. LANGE and J. H. BECHTOLD, *J. Mater. Sci.* **13** (1978) 1464.
24. H. P. KLUG and L. E. ALEXANDER, "X-ray Diffraction Procedures", (Wiley, New York, 1974). Ch. 9.
25. T. ITOH, *J. Mater. Sci. Lett.* **4** (1985) 431.
26. B. E. WARREN, "X-ray Diffraction", (Addison-Wesley, Reading, Massachusetts, 1969) Ch. 13.
27. B. E. YOLDAS, *J. Amer. Ceram. Soc.* **65** (1982) 387.
28. D. C. BRADLEY and D. G. CARTER, *Can. J. Chem.* **39** (1961) 1434.
29. *Idem, ibid.* **40** (1962) 15.
30. D. GANGULI and D. KUNDU, *J. Mater. Sci. Lett.* **3** (1984) 503.
31. D. KUNDU and D. GANGULI, *ibid.* **5** (1986) 293.
32. N. TOHGE, G. S. MOORE and J. D. MACKENZIE, *J. Non-Cryst. Solids* **63** (1984) 95.
33. R. C. MACKENZIE and G. BERGGREN, in "Differential Thermal Analysis", Vol. 1, edited by R. C. Mackenzie (Academic, London, 1970) p. 315.
34. Yu. M. POLEZHAEV, *Russ. J. Phys. Chem.* **41** (1967) 1590.
35. R. C. GARVIE, *J. Phys. Chem.* **69** (1965) 1238.
36. G. FAGHERAZZI, S. ENZO, V. GOTTARDI and G. SCRINCI, *J. Mater. Sci.* **15** (1980) 2693.
37. D. L. PORTER and A. H. HEUER, *J. Amer. Ceram. Soc.* **62** (1979) 298.
38. D. VIECHNICKI and V. S. STUBICAN, *ibid.* **48** (1965) 292.
39. C. F. GRAIN, *ibid.* **50** (1967) 288.
40. Y. MURASE, E. KATO and K. DAIMON, *ibid.* **69** (1986) 83.
41. K. S. MAZDIYASNI, in Proceedings of 6th International Symposium on Reactivity of Solids, Schenectady, 1968, edited by J. W. Mitchell, R. C. DeVries, R. W. Roberts and P. J. Cannon (Wiley, New York, 1969) p. 115.
42. H. TORAYA, M. YOSHIMURA and S. SOMIYA, *J. Amer. Ceram. Soc.* **67** (1984) C-183.



*Received 12 January*
*and accepted 15 July 1987*